Applied Physics Letters

Bi-directional superluminal ring lasers without crosstalk and gain competition

Cite as: Appl. Phys. Lett. **120**, 251105 (2022); https://doi.org/10.1063/5.0093164
Submitted: 26 March 2022 • Accepted: 16 June 2022 • Published Online: 23 June 2022

Zifan Zhou, Ruoxi Zhu, Nicholas J. Condon, et al.

AIP Publishing

Applied Physics Letters ARTICLE scitation.org/journal/apl

Bi-directional superluminal ring lasers without crosstalk and gain competition

Cite as: Appl. Phys. Lett. **120**, 251105 (2022); doi: 10.1063/5.0093164
Submitted: 26 March 2022 · Accepted: 16 June 2022 ·
Published Online: 23 June 2022

Zifan Zhou,[1,a)] Ruoxi Zhu,[1] Nicholas J. Condon,[2] Devin J. Hileman,[2] Jason Bonacum,[2] and Selim M. Shahriar[1,3]

AFFILIATIONS

[1]Department of Electrical and Computer Engineering, Northwestern University, Illinois 60208, USA
[2]Digital Optics Technologies, Rolling Meadows, Illinois 60008, USA
[3]Department of Physics and Astronomy, Northwestern University, Illinois 60208, USA

[a)]Author to whom correspondence should be addressed: zifan.zhou@northwestern.edu

ABSTRACT

In this paper, we present the experimental observation of simultaneous bi-directional superluminal lasing in a triangular ring cavity without gain competition and crosstalk as needed for realizing a gyroscope based on the Sagnac effect. The gain spectrum for each of the lasers is tailored to be a narrow dip on top of a broad gain using two stable isotopes of Rb. Specifically, we make use of ^{85}Rb to produce a broad gain spectrum via the optically pumped Raman gain process and ^{87}Rb to produce a narrow absorption spectrum via the optically pump Raman depletion process. A separate gain cell is used for the laser in each direction. Inferred from the simulation, the spectral sensitivity enhancements of the clock-wise and counter-clock-wise superluminal ring lasers are ∼362 and ∼505, respectively, with the imbalance attributed to differences in pump powers.

For a superluminal ring laser (SRL), the group velocity of light is greater than the speed of light in vacuum without violating special relativity or causality.[1] Such a laser has been shown to be more sensitive to rotations and perturbations in the cavity length than conventional lasers.[2–10] Producing a superluminal laser requires a gain medium that not only provides amplification to the laser field inside the cavity but also needs to have negative dispersion at the lasing frequency. According to the Kramers–Kronig relations,[11] the required gain spectrum needs to be a broad gain overlapping with a narrow absorption profile. Previously, we have shown single directional superluminal lasing using various approaches, including diode-pumped alkali laser (DPAL) gain combined with Raman depletion,[12] double Raman gain,[13] optically pumped Raman gain combined with self-pumped Raman depletion,[14] electromagnetically induced transparency in a Raman laser,[15] and optically pumped Raman gain combined with optically pumped Raman depletion.[16] Some applications, such as gyroscopes, require two lasers that are counter-propagating in the same cavity to operate. Moreover, bi-directional lasing that shares the same cavity longitudinal mode can eliminate common-mode classical noise. However, a key challenge in realizing two counter-propagating lasers in the same cavity is the possibility of gain competition and crosstalk. Because of this reason, it is not possible to realize such a system using the approach based on DPAL gain, since it is bi-directional. On the contrary, for a system with large Doppler broadening, such as a warm vapor cell, the Raman gain and depletion processes are very strongly unidirectional.[13] This is due to the fact that the spectral width of the two-photon Raman process (∼1 MHz) is much narrower than the Doppler broadened width (∼600 MHz at room temperature). In the frame of an atom with non-zero velocity along the direction of propagation of the optical beams, when the Raman pump is counter-propagating with respect to the Raman probe, the frequencies of the Raman pump and the Raman probe are shifted in the opposite directions. Therefore, only the atoms with velocities close to zero contribute to the Raman gain. On the contrary, when the Raman pump is co-propagating with the Raman probe, the frequencies of the Raman pump and the Raman probe are shifted in the same direction with a small difference in the frame of moving atoms. As a result, virtually all the atoms contribute to Raman gain or depletion for the probe field. Therefore, the Raman laser field produced in one direction only has vanishing small interaction with the Raman pump in the opposite direction. Consequentially, the two Raman lasers do not have any noticeable crosstalk, as confirmed in experimental observations.

The techniques we cited above for realizing superluminal gain, excluding the one based on DPAL gain, can each be used, in principle, for realizing a pair of decoupled, counter-propagating superluminal lasers. Of these techniques, the one that employs optical pumping for

both Raman gain and Raman depletion is the most flexible. In this approach, the dip-in-gain spectrum experienced by the Raman laser field can be produced over a broad range of operating parameters such as power levels and detunings of the Raman pump and the optical pump. This feature enables one to tune the parameters of the dip-in-gain profile to reach conditions that would yield higher spectral sensitivity enhancement than the other techniques.

In this paper, we demonstrate an experimental realization of two superluminal ring lasers that are counter propagating in the same cavity containing a natural mixture of two Rb isotopes, employing optically pumped Raman gain in one isotope and optically pumped Raman depletion in another. Specifically, in each direction, we first produce a conventional Raman laser in the presence of an optical pump in ^{85}Rb. Then we configure ^{87}Rb to produce optically pumped Raman depletion in the vicinity of the frequency of the Raman laser, which creates an anomalous dispersion experienced by the Raman laser field. We report estimated spectral sensitivity enhancements of the clock-wise (CW) and counter-clock-wise (CCW) superluminal ring lasers by factors of ∼362 and ∼505, respectively, with the imbalance attributed to differences in pump powers.

To produce the superluminal condition in the Raman laser, the pump lasers need to be tuned to specific frequencies. The optical fields and the relevant energy levels are shown in Fig. 1. The frequency configurations of the pump lasers for the CW direction and the CCW direction are identical. Therefore, each pump beam is shared between the two directions. For each direction, we first produce conventional Raman lasing in ^{85}Rb, as illustrated schematically in the left panel in Fig. 1. The hyperfine energy levels F = 2 and F = 3 in the $5S_{1/2}$ manifold are denoted as states $|1\rangle$ and $|2\rangle$, respectively, and F = 2 and F = 3 in the $5P_{1/2}$ manifold are denoted as states $|3\rangle$ and $|4\rangle$, respectively. The $5P_{3/2}$ manifold is considered as a single level, denoted as state $|5\rangle$, due to the fact that the energy differences between the hyperfine levels in this manifold are smaller than the Doppler broadening.

Optical pump A is tuned on resonance with the $|1\rangle \leftrightarrow |5\rangle$ transition. The atoms are excited to $|5\rangle$ by the optical pump and decay down to $|1\rangle$ and $|2\rangle$. Therefore, in the presence of the optical pump, the population of $|2\rangle$ is greater than that of $|1\rangle$. Raman pump A is tuned below the $|2\rangle \leftrightarrow |3\rangle$ transition resonance by a detuning of δ. With this configuration, a Raman laser field would be produced at the two-photon resonance frequency on the $|1\rangle \leftrightarrow |3\rangle$ and the $|1\rangle \leftrightarrow |4\rangle$ transitions, assuming the Raman gain exceeds the cavity loss, and the cavity resonance frequency is tuned to the peak of the Raman gain.

In ^{87}Rb, illustrated on the right panel of Fig. 1, the hyperfine energy levels F = 1 and F = 2 in the $5S_{1/2}$ manifold are denoted as states $|1\rangle$ and $|2\rangle$, respectively, and F = 1 and F = 2 in the $5P_{1/2}$ manifold are denoted as states $|3\rangle$ and $|4\rangle$, respectively. Just as in the case of ^{85}Rb, the $5P_{3/2}$ manifold is considered as a single level, denoted as state $|5\rangle$. Optical pump B and Raman pump B are configured to produce Raman depletion in the Raman laser field produced in ^{85}Rb isotope. Specifically, optical pump B is tuned to be resonant with the $|2\rangle \leftrightarrow |5\rangle$ transition to produce population difference between $|1\rangle$ and $|2\rangle$. Raman pump B is tuned below the $|2\rangle \leftrightarrow |3\rangle$ resonance by a detuning of δ'.

To align the center frequency of the Raman depletion process with the frequency of the Raman laser, which is denoted as f_L, it is necessary to ensure that $\delta' = \delta + 2.28$ GHz. As such, the frequency of Raman pump B, denoted as f_{RPB}, can be related to the frequency of Raman pump A, f_{RPA}, as $f_{RPA} - f_{RPB} = F_{87} - F_{85} = 3.799$ GHz, where F_{85} and F_{87} are the hyperfine splitting frequencies between states $|1\rangle$ and $|2\rangle$ in ^{85}Rb and ^{87}Rb, respectively. To realize such relations accurately in the experiment, we make use of an offset phase lock servo (OPLS) to lock the frequency and the phase of Raman pump B to Raman pump A. In the presence of the Raman depletion produced in this manner, the superluminal condition is, thus, created for the Raman laser. By tuning the parameters in the experiment, such as the temperature of the Rb cells and the powers and detunings of the Raman pumps and the optical pumps, the sensitivity enhancement factor can be modified and optimized.

The schematic of the experimental configuration is illustrated in Fig. 2. The cavity is an acute isosceles triangle and is composed of two

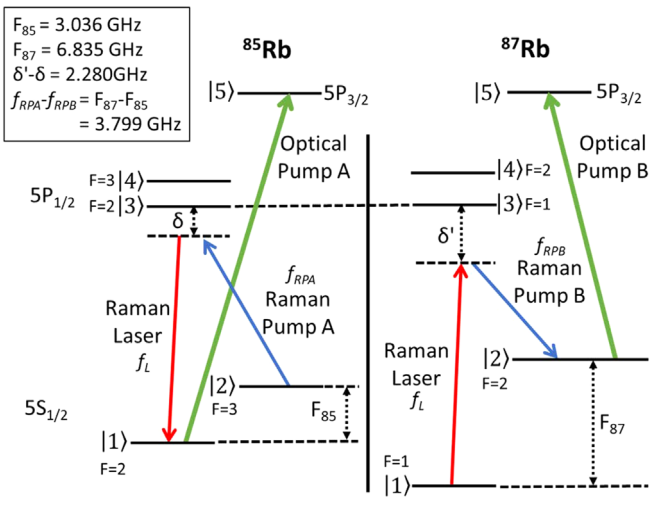

FIG. 1. Schematic of the optical fields and the relevant energy levels in the Rb vapor cells.[17]

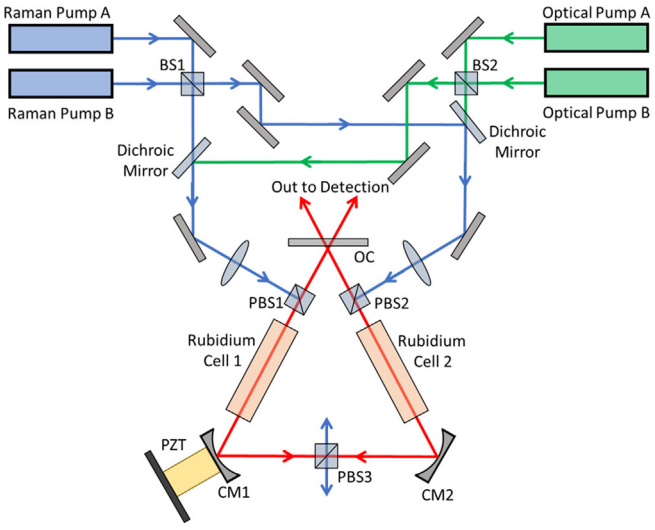

FIG. 2. Schematic of the cavity used to generate simultaneous bi-directional superluminal lasing. BS1 and BS2 are non-polarizing beam splitters, and each has an ideal split ratio of 50/50.

high reflectivity concave mirrors and one output coupler. The output coupler (OC) is flat and has a reflectivity of 71%. One of the concave mirrors is attached to a piezoelectric transducer (PZT), which can be used to produce a small perturbation in the cavity length. The two Rubidium vapor cells, which contain natural Rubidium mixtures, are placed in the equal sides of the cavity and thermally stabilized at 80 °C. The vertically polarized pump lasers are coupled into the cavity through polarizing beam splitters (PBSs), producing horizontally polarized Raman lasing. The optical pumps are combined with the Raman pumps through dichroic mirrors before entering the cavity, and their polarizations are tuned to be the same as that of the Raman pumps. BS1 and BS2 are non-polarizing beam splitters with an ideal split ratio of 50/50 that are used for combining the pump beams as well as splitting the pump beams for the two directions. PBS1 and PBS2 in Fig. 2 are used to couple the pump lasers for producing the counterclockwise (CCW) and clockwise (CW) direction Raman lasing, respectively. PBS3 is used to remove the pump beams from the cavity in order to prevent them from entering the second cell. Even though the Raman laser produced in one of the vapor cells passes through the other cell, the two-photon effect caused by the Raman pump in the opposite direction is negligible, as discussed previously. All the pump beams are focused to match the cavity mode. The outputs of the two Raman lasers are combined outside the cavity using a non-polarizing beam splitter and received by a high-speed photo detector for measuring the beat-signal.

We have used a semi-classical theoretical model to determine the expected behavior of the superluminal lasers generated in this manner. In this model, we solve the density matrix equations of motion for the Rb atoms for both isotopes and the equation of motion for a single mode laser in a self-consistent manner[18,19] for each direction. Using an iterative process, as described in detail in Ref. 19, we can find the frequency as well as the intensity of the laser field produced in steady state for a given set of parameters.

The representations of the atom–field interactions in both isotopes employed in the theoretical model are illustrated in Fig. 3. In each isotope, the states designated as $|1\rangle$, $|2\rangle$, $|3\rangle$, and $|4\rangle$ are as defined earlier. The Raman pump fields have the Rabi frequency of Ω_{RPA} and Ω_{RPB}, which can be calculated from the intensities of the applied laser beams. For simplicity, we consider the optical pumping in each of the two isotopes as an effective one-way decay rate, denoted as Γ_{OPA} and Γ_{OPB}, between the two hyperfine levels in the $5S_{1/2}$ manifold. The effective decay rates due to optical pumping are calculated individually using two auxiliary three-level models, one for each isotope. The Doppler effect is taken into account in these models, since the optical pumping process is sensitive to the Doppler shift, unlike co-propagating Raman transitions. Details of the approach used for calculating this effective decay rate as well as justification of the validity for this approach can be found in Ref. 17.

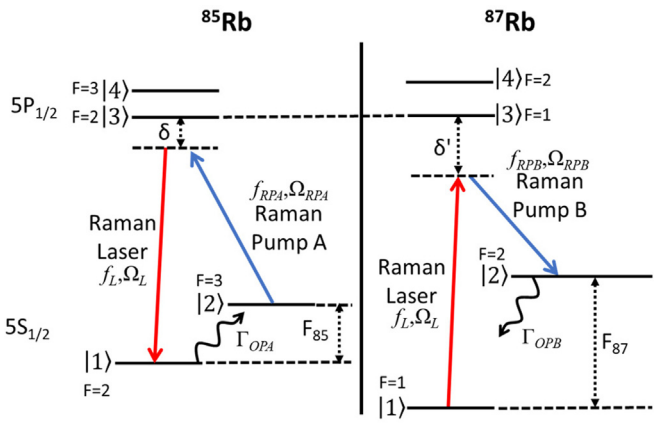

FIG. 3. Schematic of optical fields and relevant energy levels of the theoretical model.

It is important to note that the atomic decay from the excited states ($|3\rangle$ and $|4\rangle$) and the collisional decay between the ground states ($|1\rangle$ and $|2\rangle$) are not shown in the diagram, but they are taken into consideration in the simulation. With given parameters, namely, the frequency and the field amplitude for the Raman laser, the algorithm solves the Liouville equation in steady state and finds the net susceptibility that is experienced by the Raman laser field due to interactions with both isotopes, weighted by the natural abundance. The laser equations are then used to check whether these parameters along with the calculated susceptibility together satisfy the lasing condition. This process is iterated until convergence is achieved to a chosen degree of precision, thereby determining the frequency, f_L, and the Rabi frequency, Ω_L, of the Raman laser field in steady state.

The experimental observation of the output power of the Raman lasers as functions of the frequency of the Raman pump B (i.e., f_{RPB}) is shown in Fig. 4. The frequencies of Raman pump A in both directions are fixed to specific values. The frequency of Raman pump B for each direction is scanned via tuning the reference frequency of the corresponding offset phase lock servo (i.e., OPLS). The center frequency in these figures, f_0, is the frequency of Raman pump B when the difference between the frequencies of Raman pumps A and B is 3.799 GHz, which is the difference between the hyperfine splittings of the two

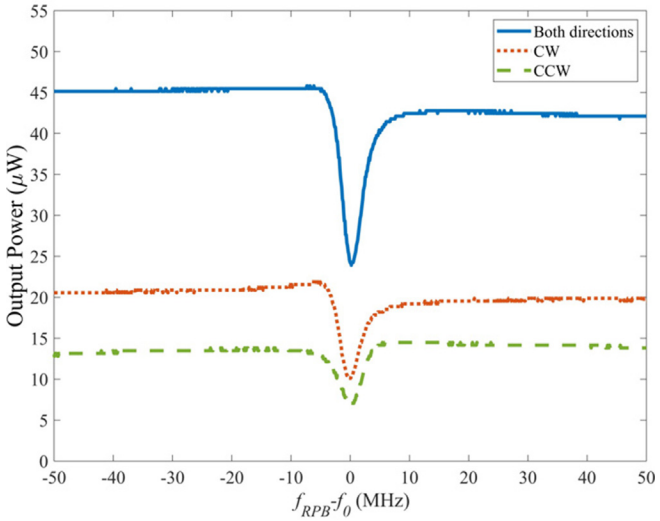

FIG. 4. Output power of the bi-directional Raman laser as a function of the frequency of Raman pump B. Here, the center frequency, f_0, is the frequency of Raman pump B when the difference between the frequencies of Raman pumps A and B is 3.799 GHz, which is the difference between the hyperfine splittings of the two isotopes.

isotopes. The total power, for both directions, of Raman pump A and Raman pump B are 4 and 2 mW, respectively. The total power, for both directions, of optical pump A and optical pump B are 175 and 70 mW, respectively. The ratio of the effective powers for each of these lasers for each direction is ideally unity; however, in practice, this ratio is expected to differ from the ideal value due to different propagation lengths and optical components for the two paths. As such, we use the ratio as a fitting parameter, r, defined as the ratio between the CCW and CW powers for all the pump lasers.

The solid trace is the combined output power of the bi-directional Raman lasers. The dotted line and the dashed line are the output power of the CW laser and the CCW laser, respectively. Due to the imperfection in the beam splitters used to separate pump beams for the two directions, the output power of the CW and the CCW are slightly different. As can be seen, the Raman lasers in both directions experience depletion in the vicinity of the two-photon resonance. Thus, at the center of the depletion, the laser field should be experiencing negative dispersion, which leads to superluminal lasing.

The corresponding simulation results are shown in Fig. 5. Here, we use the experimental parameters to generate the output power as a function of f_{RPB} to match the experimental data. In the simulation, as fitting parameters, we varied the temperature of the Rb cell slightly and adjusted the focused beam diameters of each of the four pump lasers. The quantity r defined above, which represents the ratio between the pump powers for the two directions, is also treated as a fitting parameter. The temperature used for generating Fig. 5 is 79.83 °C. The power ratio between the pump beams for the CCW direction and the CW direction is ∼0.643. In Fig. 5(b), we generate the sensitivity enhancement of such lasers at the center of the dip shown in Fig. 5(a). As can be seen, the sensitivity enhancement of the CW direction laser reaches ∼505 in the center and that of the CCW laser is as high as ∼362. Determining the value of the sensitivity enhancement factor experimentally is very difficult for our current experimental setup, since it would require extreme stability against various sources of fluctuations. Efforts are under way to build a robust version of this apparatus, mounted on an invar plate, and encased inside a vacuum chamber.

The losses in the cavity are crucial for applications such as gyroscopes. There are three important types of losses in a ring laser gyroscope containing a gain medium in a glass cell inside the cavity. The first is the finite transmissivity of the output coupler. The second is un-mode-matched reflection from windows of the glass cell. The third is residual scattering from the glass cell windows as well as the cavity mirrors. To see how the loss parameters affect the sensitivity of the superluminal RLG, we assume, for example, that some mechanism (such as dithering) is used to overcome the lock-in effect,[20] and the Schawlow–Townes linewidth (STL) of the laser remains unaffected by superluminal enhancement.[21] Under these assumptions, the minimum measurable rotation rate is determined by the minimum measurable beat frequency. This, in turn, is given by twice the geometric mean of the measurement bandwidth (i.e., the inverse of the signal integration time, τ) and the Schwalow–Townes linewidth (STL)[22] of the laser in each direction, assuming them to be the same. Thus, the minimum measurable linewidth is given by $\Delta f_{\min} = \sqrt{hf/\pi P_o \tau_C^2 \tau}$. The sum of losses affects this quantity in two different ways. First, for a given threshold gain, the output power is smaller for higher losses. Second, the cavity decay time becomes smaller with increasing losses. For the system reported here, we have not yet carried out a systematic investigation of what the values of these residual loss parameters are. Such a study would be carried out in the future.

To summarize, in this paper, we reported the demonstration of simultaneous bi-directional superluminal lasing in a single cavity. The technique we have employed makes use of optically pumped Raman gain in one isotope of rubidium and optically pumped Raman depletion in another isotope of rubidium. A separate gain cell is used for the laser in each direction. No gain competition between the two lasers is observed due to the extreme unidirectionality of the Raman gain and depletion processes. From the theoretical model we developed, we infer that the sensitivity enhancement factors in the CW and CCW directions are ∼505 and ∼362, respectively. This demonstration paves

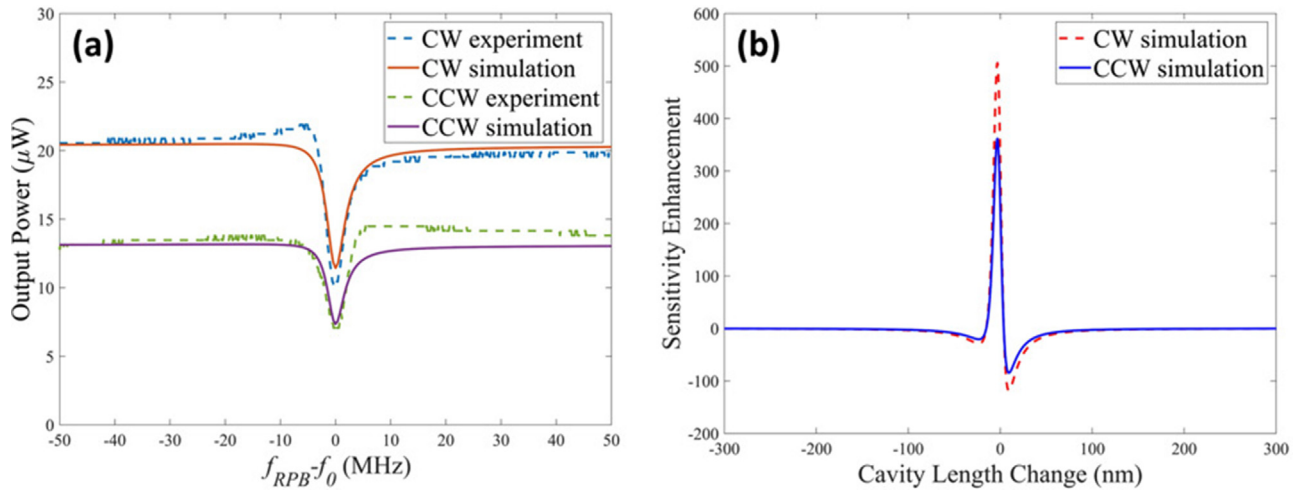

FIG. 5. Simulation results[17] of (a) the output power of the bi-directional Raman laser as a function of the frequency of Raman pump B and (b) corresponding sensitivity enhancement when the lasers are operating at the center frequency shown in Fig. 5(a).

the way for realizing an ultra-sensitive superluminal ring laser gyroscope employing the scheme presented here.

This work was supported by Air Force Office of Scientific Research (Nos. FA9550-18-01-0401 and FA9550-21-C-0003) and Defense Security Cooperation Agency (No. PO4441028735).

AUTHOR DECLARATIONS

Conflict of Interest

The authors have no conflicts to disclose.

Author Contributions

Zifan Zhou: Data curation (equal); Formal analysis (equal); Visualization (equal); Writing – original draft (equal). **Ruoxi Zhu:** Formal analysis (equal). **Nicholas J. Condon:** Data curation (equal). **Devin J. Hileman:** Data curation (equal). **Jason Bonacum:** Formal analysis (equal). **Selim M. Shahriar:** Conceptualization (equal); Formal analysis (equal); Funding acquisition (equal); Methodology (equal); Project administration (equal); Supervision (equal); Validation (equal); Writing – review and editing (equal).

DATA AVAILABILITY

The data that support the findings of this study are available from the corresponding author upon reasonable request.

REFERENCES

[1]L. J. Wang, A. Kuzmich, and A. Dogariu, "Gain-assisted superluminal light propagation," Nature **406**(6793), 277–279 (2000).
[2]H. N. Yum, M. Salit, J. Yablon, K. Salit, Y. Wang, and M. S. Shahriar, "Superluminal ring laser for hypersensitive sensing," Opt. Express **18**(17), 17658–17665 (2010).
[3]M. S. Shahriar, G. S. Pati, R. Tripathi, V. Gopal, M. Messall, and K. Salit, "Ultrahigh enhancement in absolute and relative rotation sensing using fast and slow light," Phys. Rev. A **75**, 053807 (2007).
[4]G. S. Pati, M. Salit, K. Salit, and M. S. Shahriar, "Demonstration of displacement-measurement-sensitivity proportional to inverse group index of intracavity medium in a ring resonator," Opt. Commun. **281**, 4931–4935 (2008).
[5]G. S. Pati, M. Salit, K. Salit, and M. S. Shahriar, "Demonstration of a tunable-bandwidth white light interferometer using anomalous dispersion in atomic vapor," Phys. Rev. Lett. **99**, 133601 (2007).
[6]M. S. Shahriar and M. Salit, "Application of fast-light in gravitational wave detection with interferometers and resonators," J. Mod. Opt. **55**, 3133 (2008).
[7]D. D. Smith, H. Chang, L. Arissian, and J. C. Diels, "Dispersion-enhanced laser gyroscope," Phys. Rev. A **78**, 053824 (2008).
[8]D. D. Smith, K. Myneni, J. A. Odutola, and J. C. Diels, "Enhanced sensitivity of a passive optical cavity by an intracavity dispersive medium," Phys. Rev. A **80**, 011809(R) (2009).
[9]D. D. Smith, H. Chang, K. Myneni, and A. T. Rosenberger, "Fast-light enhancement of an optical cavity by polarization mode coupling," Phys. Rev. A **89**, 053804 (2014).
[10]O. Kotlicki, J. Scheuer, and M. S. Shahriar, "Theoretical study on Brillouin fiber laser sensor based on white light cavity," Opt. Express **20**(27), 28234 (2012).
[11]H. N. Yum and M. S. Shahriar, "Pump–probe model for the Kramers–Kronig relations in a laser," J. Opt. **12**, 104018 (2010).
[12]J. Yablon, Z. Zhou, M. Zhou, Y. Wang, S. Tseng, and M. S. Shahriar, "Theoretical modeling and experimental demonstration of Raman probe induced spectral dip for realizing a superluminal laser," Opt. Express **24**, 27444–27456 (2016).
[13]Y. Wang, Z. Zhou, J. Yablon, and M. S. Shahriar, "Effect of multiorder harmonics in a double-Raman pumped gain medium for a superluminal laser," Opt. Eng. **54**(5), 057106 (2015).
[14]Z. Zhou, M. Zhou, and M. S. Shahriar, "Superluminal Raman laser with enhanced cavity length sensitivity," Opt. Express **27**, 29738–29745 (2019).
[15]Y. Sternfeld, Z. Zhou, J. Scheuer, and M. S. Shahriar, "Electromagnetically induced transparency in Raman gain for realizing a superluminal ring laser," Opt. Express **29**, 1125–1139 (2021).
[16]Z. Zhou, N. Condon, D. Hileman, and M. S. Shahriar, "Observation of a highly superluminal laser employing optically pumped Raman gain and depletion," Opt. Express **30**, 6746 (2022).
[17]Z. Zhou, N. J. Condon, D. J. Hileman, S. C. Tseng, and S. M. Shahriar, "Realization of bi-directional superluminal ring lasers using adjacent transitions in two isotopes of rubidium," in *Frontiers in Optics + Laser Science 2021, Technical Digest Series* (Optica Publishing Group, 2021), Paper No. JTh5A.25.
[18]Z. Zhou, J. Yablon, M. Zhou, Y. Wang, A. Heifetz, and M. S. Shahriar, "Modeling and analysis of an ultra-stable subluminal laser," Opt. Commun. **358**, 6–19 (2016).
[19]M. S. Shahriar, Y. Wang, S. Krishnamurthy, Y. Tu, G. S. Pati, and S. Tseng, "Evolution of an N-level system via automated vectorization of the Liouville equations and application to optically controlled polarization rotation," J. Mod. Opt. **61**(4), 351–367 (2014).
[20]W. W. Chow, J. Gea-Banacloche, L. M. Pedrotti, V. E. Sanders, W. Schleich, and M. O. Scully, "The ring laser gyro," Rev. Mod. Phys. **57**, 61 (1985).
[21]J. Scheuer and M. S. Shahriar, "Lasing dynamics of super and sub luminal lasers," Opt. Express **23**, 32350–32366 (2015).
[22]T. Dorschner, H. Haus, M. Holz, I. Smith, and H. Statz, "Laser gyro at quantum limit," IEEE J. Quantum Electron. **16**(12), 1376–1379 (1980).